International Forum on Aeroelasticity and Structural Dynamics
IFASD 2019
9-13 June 2019, Savannah, Georgia, USA

FAST FLUID-STRUCTURE COMPUTATIONAL METHOD TAKING INTO ACCOUNT NON-LINEAR AERODYNAMIC

B.Barriety[1], J-P. Boin[1] , O. Chandre-Vila[1] and T.Mauermann[2]

[1] Loads and Aeroelasticity Department, AIRBUS OPERATIONS SAS
316, Route de Bayonne, 31060 Toulouse, France
bernard.barriety@airbus.com
jean-philippe.boin@airbus.com

[2] Overall Aircraft Design, AIRBUS OPERATIONS SAS
316, Route de Bayonne, 31060 Toulouse, France
tobias.mauermann@airbus.com

Keywords: static aeroelasticity, non-linear aerodynamics, rapid method, transonic.

Abstract: Current fast static aeroelasticity methods are mainly based on a linear formulation. These approaches are unable to predict the non-linear behavior of the aerodynamic for transonic flows. In consequence, many assumptions are needed to provide artificially a non-linear behavior. Nevertheless, flight tests and wind tunnel tests have shown that the corrected linear approach is not sufficiently accurate in the non-linear flow regime. Today, the state of the art in static Aeroelasticity for predicting the aerodynamic non-linearities is to run CFD/CSM. This approach is costly in term of modeling and computational time. On top of that, CFD is not able to cover with accuracy the complete aircraft flight domain, which prevents to use CFD/CSM in a regular way for the aircraft Load analysis.

The aim of this study is to predict the static aeroelasticity effects acting on an aircraft, taking into account the aerodynamic non-linearities, with a rapid and robust method based on the principle of the local incidence shift. Due to external loading during flight, the flexible wing is affected by the structural deformation which leads to a variation of the local incidence of each wing section. As a consequence, the aerodynamic characteristics of each section will change accordingly.

First, the general principle of the fast fluid-structure method is shown. Then a validation of the method using Wind Tunnel Tests and high fidelity CFD/CSM calculations is presented. Finally, a way of using this new method in an industrial context is proposed.

NOMENCLATURE

CFD	Computational Fluid Dynamics
CSM	Computational Structure Mechanics
FEM	Finite Element Model
VLM	Vortex Lattice Method
AIC	Aerodynamic Influence Coefficient
WTT	Wind Tunnel Test
AoA	Angle of Attack
θ, θ_{twist}	Twist distribution
η	Reduced span
α_{eff}	Effective angle of attack
α_{geo}	Geometric angle of attack
α_{ind}	Induced angle of attack
U_∞	Free stream velocity
K_z	Local lift coefficient
$\Delta\alpha_{flex}$, $\delta\alpha_{flex}$	Local incidence shift
$\mathbf{u}$	Structural deformation vector
$\mathbf{Q}$	AIC matrix
$\mathbf{S}$	Summation matrix
$[\mathbf{K}]$, $\mathbf{K}$	Stiffness matrix
$[\mathbf{K^{-1}}]$	Flexibility matrix
k	Relaxation factor
$P(\mathbf{u})$	External loads
$\bar{q}$	Dynamic pressure

1 INTRODUCTION

At each phase of the aircraft development, the static aeroelasticity effects have a big impact on the aircraft design. First, it modifies the global aircraft behaviour which has a direct impact on the design of the control surfaces and the design of the control laws. These static aeroelasticity effects are also at the origin of the passive loads alleviation which contribute to the weight reduction of the aero structures. Finally it plays a significant role in the performance of the aircraft for off-design conditions. So, static aeroelasticity effects must be taken into account in a more accurate and robust way.
The aim of this study is to predict the static aeroelasticity effects acting on an aircraft, taking into account the aerodynamic non-linearities, with a rapid and robust method based on the principle of the local incidence. Due to the external forces loading during the flight, the flexible wing is affected by the structural deformation which leads to a variation of the local incidence of each wing section. As a consequence, the aerodynamic characteristics of each section will change accordingly. It impacts the local distribution of the aerodynamic loads, the aircraft loads, the global behavior of the aircraft, its stability and controllability and the aerodynamic performance.

Current fast static aeroelasticity methods are mainly based on a linear formulation [3]. These approaches are unable to predict the non-linear behavior of the aerodynamic for transonic flows. In consequence, many assumptions are needed to provide artificially a non-linear behavior. The most current approach is to correct the linear method for the compressibility effects using non-linear aerodynamic database such as CFD for instance. These corrections are usually applied to the Aerodynamic Influence Coefficient (AIC) matrix in order to retrieve the local lift gradients over a grid of Mach numbers. Thus, only the non-linearities due to compressible effects can be captured; non-linear effect due to viscosity are not taken into account. Nevertheless, flight tests and wind tunnel tests have shown that the corrected linear approach is not sufficiently accurate in the non-linear flow regime where viscosity and separation can play a key role.
Today, the state of the art in static Aeroelasticity for predicting the aerodynamic non-linearities is to run CFD/CSM calculation (non-linear Navier-Stokes equations solved with a RANS simulation and coupled with structural solvers). This approach is costly in term of modeling (CFD mesh generation & coupling) and computational time. Today, the CFD limitations (robustness and capability to cover with accuracy the complete aircraft flight domain), prevent to use CFD/CSM in a regular way for the aircraft Load analysis. New rapid approaches have been proposed to take benefit of the two methods linear and CFD in a coupled process. These methods are based on 2D or 2.5D CFD viscous solver coupled with a lifting surface method, [4], [5]. The effective incidence seen by each section in span is de-composed into a global incidence, a twist effect and an induced incidence, due to 3D aerodynamic effects. This induced incidence is calculated using an iterative coupling between the lifting surface prediction and the prediction of the viscous method. These methods allow to retrieve the aerodynamic on a 3D surface for a given twist or directly in a static aeroelasticity coupling where the twist is deformed according to the surface stiffness. In his paper, Agostinelli [1] proposes to use directly pre-computed section polars calculated by a 3D viscous method, similar methods for Unsteady Aerodynamics could be found in Cesnik and al. [7]. In that case, the 3D induced effect due to the rigid twist is already taken into account in the viscous polar database. The variation of this induced incidence due to the structural deformation is then estimated using a lifting surface method. In his method, more than one reference twist for the viscous polars is needed to achieve a good accuracy.
The present method is also based on 3D viscous polars given for a fixed rigid shape. But, the induced incidence variation is not calculated separately from the direct effect of the structural

deformation. Instead, a Vortex Lattice Method (VLM) is used to estimate the combined effect. This method gives already a very good accuracy with only one reference rigid shape of the clean wing (without control surface). The method can be extended to a full aircraft configuration, including control surfaces, with a moderate effort.

2 LOCAL INCIDENCE FORMULATION

2.1 Experimental results

Wind tunnel test (WTT) were performed on a "rigid model" which could be equipped with two different "rigid wing shapes" (a common plan-form for both wings but one wing was representative of the cruise twist shape named 1G and the second one had a twist shape representative of a high loaded manoeuver flight point named 2.5G). A representation of the delta of twist between the two wing shapes along the span is provided on the Figure 5, red curve "twist deformation".

Considering these wind tunnel test results and neglecting the WTT measurements oscillations at high Angle of Attack as well as the residual impact of the wing tunnel model stiffness, it is possible to observe that:

- whatever the number of Mach (from low subsonic to high transonic), the local lift coefficient and the local pitching moment coefficient for all the sections along the wing span could be deduced from one shape by applying a delta of Angle Of Attack (AoA).
- this delta of AoA could reasonably be considered as constant for each section whatever the AoA (Figure 1)
- so, this delta of AoA could reasonably be estimated in the linear zone and then propagated to the full AoA range
- this delta of AoA seems linked and more or less proportional to the delta of twist between the two wing shapes
- the non-linear onset is driven by the same level of local lift for the both shapes (which is fully consistent with assumptions currently used in static Aeroelasticity)

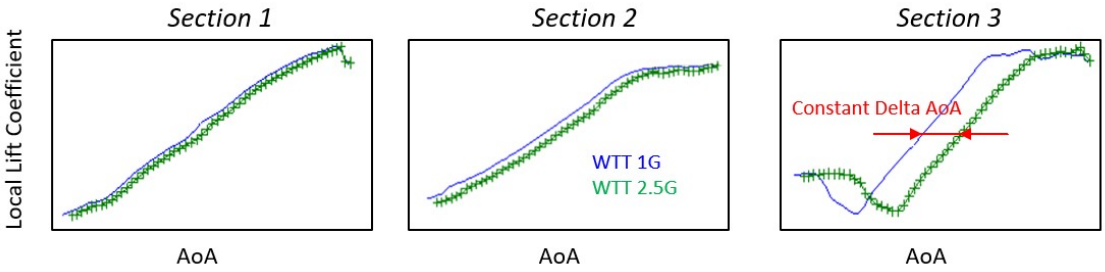

Figure 1 : WTT results: Local lift coefficient vs wing sections for two twist shapes

The next step is to propose a simple and accurate mathematical formulation of this observed delta of AoA.

2.2 Local incidence modelling

Considering a wing with a given twist distribution θ as function of the reduced span η; the effective angle of attack seen by a wing section is given by:

$$\alpha_{eff}(\eta) = \alpha_{geo} + \theta_{twist}(\eta) + \alpha_{ind}(\eta) \quad (1)$$

α_{geo} geometric angle of attack
θ_{twist} twist due to wing shape
α_{ind} induced angle of attack

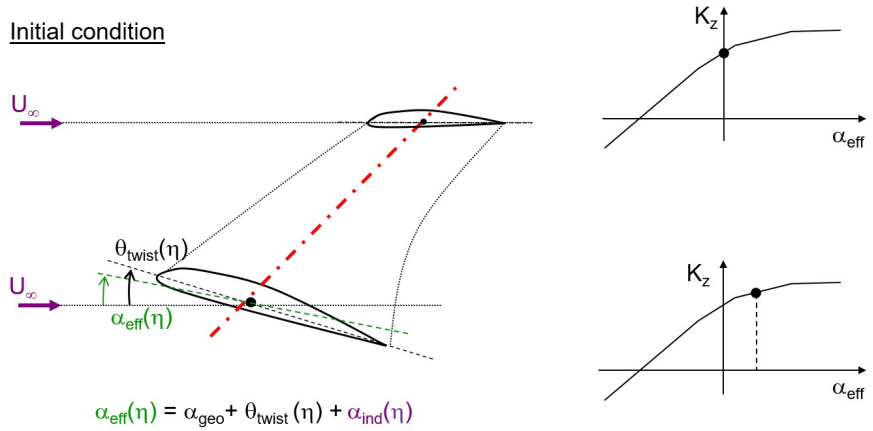

Figure 2 : Effective angle of attack definition at initial state

When the wing is deformed, the additional twist $\Delta\theta_{flex}$ causes a change in induced angle of attack and consequently section angle of attack:

$$\Delta\alpha_{flex}(\eta) = \Delta\theta_{flex}(\eta) + \Delta\alpha_{ind}(\eta) \quad (2)$$

coupled 3D effect

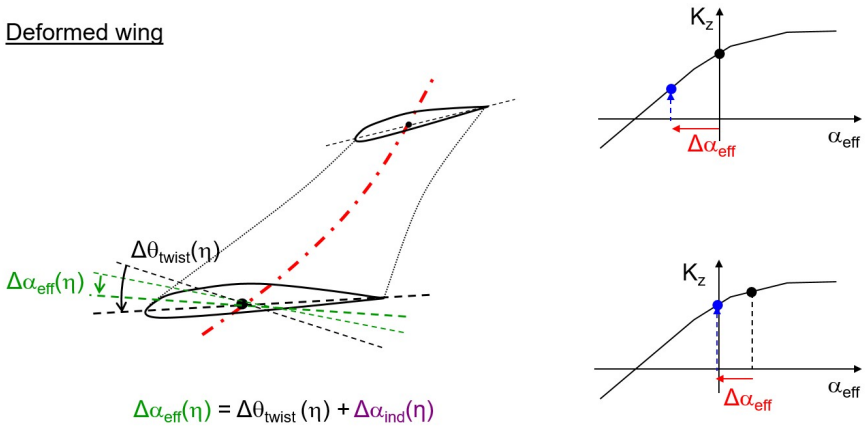

Figure 3 : Variation of the effective angle of attack for a deformed wing

For full aircraft configurations, it is difficult to isolate the local change of induced angle of attack, so the new flexibilization method approximates the combined effect $\Delta\alpha_{flex}$.

First, the local load increment due to the structural deformation **u** is calculated using the standard VLM (Figure 4) AIC matrix **Q** and a strip summation matrix **S**.

$$\delta k_z = SQu \tag{3}$$

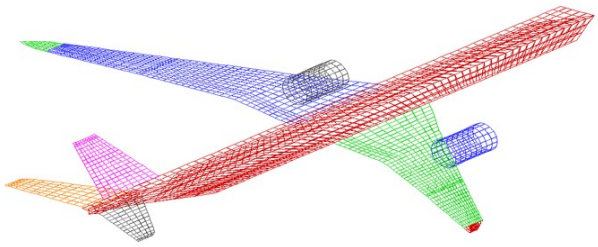

Figure 4 : VLM grid

Second, the change of the effective angle of attack ($\delta\alpha_{flex}$) is approximated by dividing the local load increment by the local average (leading region LR) lift curve slope:

$$\delta\alpha_{\text{flex}}(\eta) \approx \frac{\delta k_z(\eta)}{\left(\frac{\partial k_z}{\partial \alpha}(\eta)\right)_{\text{LR}}} \tag{4}$$

This local leading region lift curve slope is approximate with the VLM by multiplying the AIC matrix by the unitary downwash vector **{1}**:

$$\left(\frac{\delta k_z}{\delta \alpha}(\eta)\right)_{LR} = SQ\{1\} \tag{5}$$

Then the final formula for the local incidence shift due to deformation is:

$$\delta\alpha_{flex}(\eta) \approx \frac{SQu}{SQ\{1\}} \tag{6}$$

3 VALIDATION AGAINST WIND TUNNEL TEST RESULTS

The final formulation of the local incidence shift (6) was tested against the Wind Tunnel Test results already presented in the § 2.1.

For that case, the input is the delta of twist between the two wing rigid shapes and the delta alpha was calculated in accordance with the proposed formulation (6).
A plot of the delta of twist versus the wing span between the two shapes (twist 2.5G shape - twist 1G shape) and the calculated $\delta\alpha_{flex}$ is provided in the Figure 5.
Some comments concerning this plot:

- $\delta\alpha_{flex} \neq 0$ at wing root which is in line with the WTT results even if the delta of twist between the both wings is equal to 0. This is an effect of the induced incidence.
- $\delta\alpha_{flex}$ increasing with the increase of Twist deformation
- $\delta\alpha_{flex} \neq$ of the twist deformation at the wing tip which is in line with the WTT results

The difference between the delta twist and $\delta\alpha_{flex}$ is the consequence of the 3D effect on the induced angle of attack.

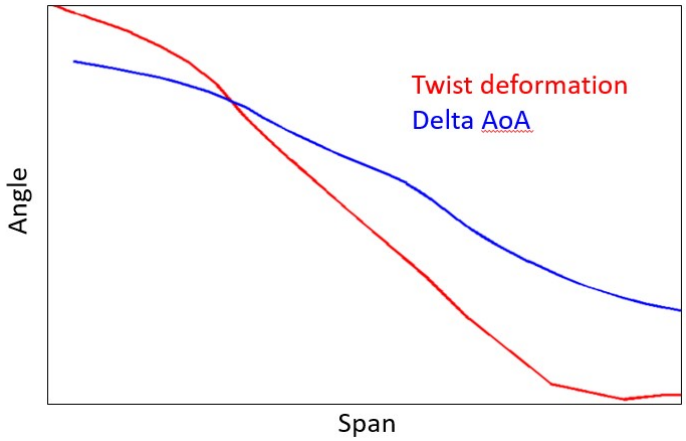

Figure 5 : Twist deformation and resulting delta-local incidence along span

The target is to apply the calculated $\delta\alpha_{flex}$ to the local lift and local pitching moment coefficient of the WTT 1G shape in order to predict the non-linear local lift and pitching moment for the WTT 2.5G shape.

The result of this comparison, whatever the tested Mach number, shows an accurate prediction of the non-linear aerodynamic behavior of the WTT 2.5G shape (Figure 6 & Figure 7 for a cruise Mach number). Especially, the onset of the non-linearity is well captured by the rapid method.

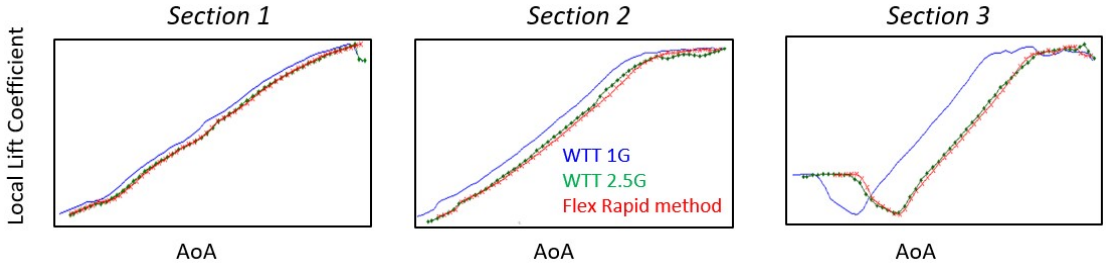

Figure 6 : Local lift distribution, comparison with wind tunnel tests results

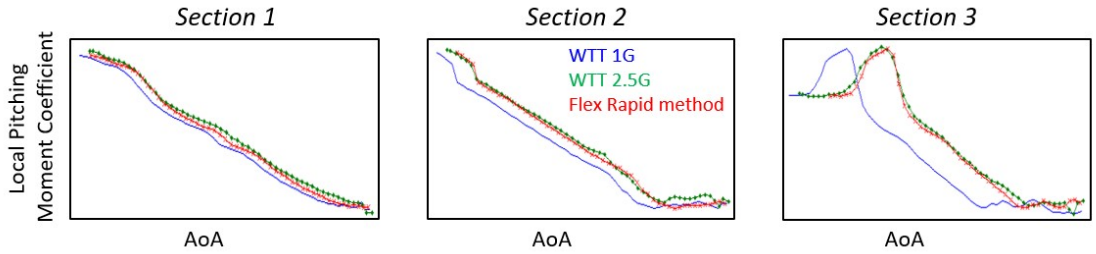

Figure 7 : Local pitching moment distribution, comparison with wind tunnel tests results

4 DEPLOYMENT OF THE METHOD IN AN AEROELASTIC COUPLING

In the previous chapter, it has be shown that it was possible to retrieve the local loads on any shape knowing the local loads on a reference shape. The method is also very quick; in the order of some milliseconds. This method could be introduced easily in a static aeroelasticity loop, Figure 8.

In a preparation phase, the local load polars are created using any kind of aerodynamic methods (CFD, WTT…). The data are stored in look-up tables (alpha-carpet) as function of Mach, Angle of Attack and reduced span of the wing. In the following examples, the structural model is a condensed stiffness model which represent the wing as a simple line of nodes. The condensed stiffness model is clamped (usually in the center wing box area) and a flexibility matrix is calculated.

The aeroelastic loop is initiated with the same global state (incidence, Mach) for each section of the wing. The calculation of the rigid aerodynamic local loads is done by interpolation inside the alpha-carpet. These local loads are then integrated and mapped to the nodes of the structural model. The deformations are computed using the flexibility matrix. Then the local $\delta\alpha_{flex}$ is computed for each section of the wing using equation (6) and a new aerodynamic loading is interpolated for the next iteration. The deformation calculated with the flexibility matrix corresponds to the deformation between an unloaded wing (Jig shape) and the deformed wing under the current loading conditions (Flight shape). To work properly, the $\delta\alpha_{flex}$ must be calculated with the deformation between the shape used as reference for the creation of the alpha-carpet (Reference shape) and the Flight shape. In case the Reference shape is not a Jig shape, the deformation between these two shapes have to be removed from the total Jig to Flight deformation, in order to get the Reference to Flight deformation. As any classical aeroelastic loop, the iterations are stopped when a convergence criteria is reached. For instance when the deformation between two iteration is lower than a given threshold.

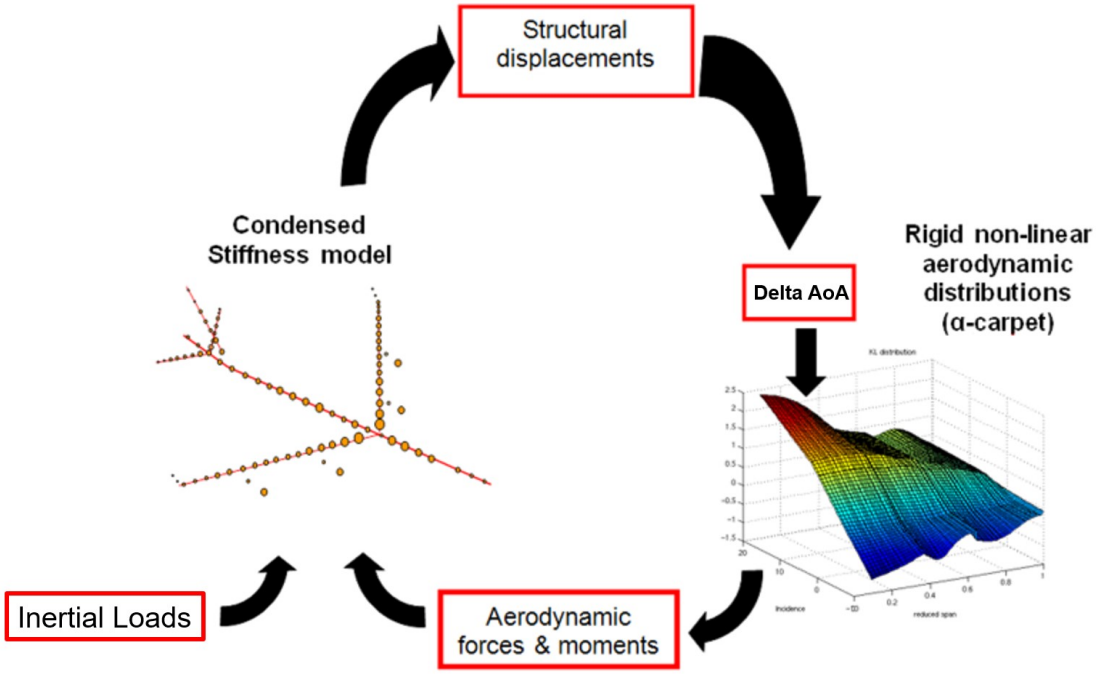

Figure 8 : Static aeroelasticity loop

The linear static aeroelasticity loop as any linear iterative problem could be solved directly with an implicit form. The final deformation **u** is directly a function of the initial step $\mathbf{u}_0$ and a combination of the linear functions, written as a matrix product.
In the case of non-linear problems, such as CFD/CSM, the iterative process is solved with an explicit scheme stabilized using a relaxation factor k, Figure 9. The process is initialized with a null vector of deformation, $\mathbf{u}_0=0$. P(**u**) denotes the external loads (aerodynamic and inertial) function of the deformation, $\mathbf{[K^{-1}]}$ is the flexibility matrix. The static equilibrium point is the root of the function $f(\mathbf{u})=\mathbf{u}-\mathbf{[K^{-1}]}.P(\mathbf{u})$.

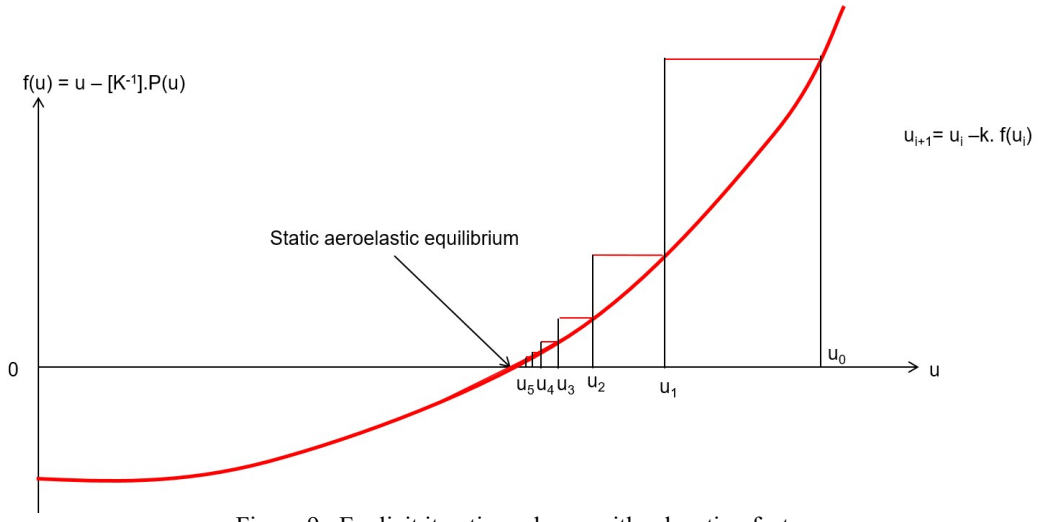

Figure 9 : Explicit iterative scheme with relaxation factor

In order to improve the convergence and the robustness, a Newton step algorithm has been implemented, Figure 10. For that method, the derivative of the function P(**u**) is needed. This derivative is approximated using the AIC matrix.

$$P(u) \approx \bar{q}Qu; P'(u) \approx \bar{q}Q \tag{7}$$

The deformation at iteration i+1 is approximated by:

$$u_{i+1} = u_i - (K - \bar{q}Q)^{-1}(Ku_i - P(u)) \tag{8}$$

This approximation helps only the convergence of the algorithm but doesn't change the value of the final result.

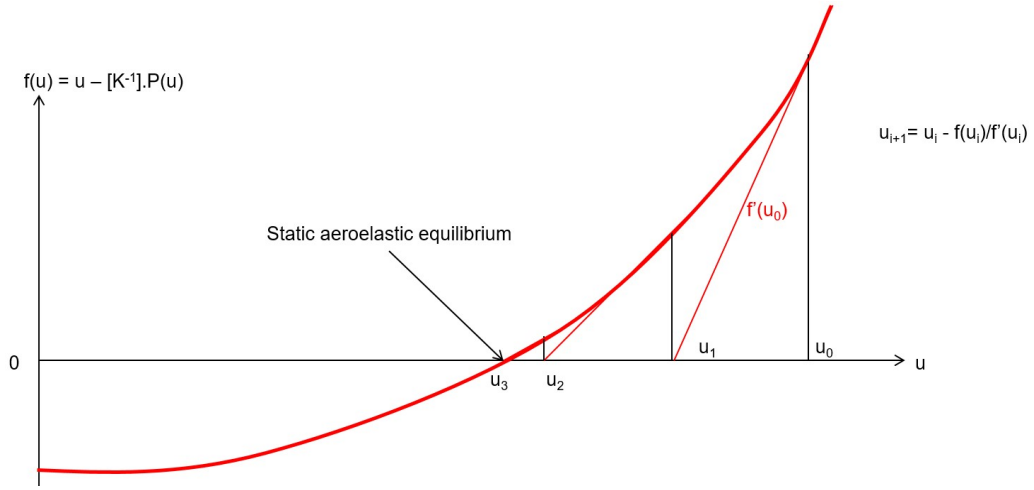

Figure 10 : Newton step algorithm

5 VALIDATION AGAINST CFD/CSM RESULTS

In this section the results of an aeroelastic coupling using the fast method are compared with high fidelity CFD/CSM results. In a preparation phase, CFD is used to build all the needed polars for a given reference shape (rigid) corresponding more or less to the cruise shape. The alpha-carpet is built for a transonic Mach number above 0.8 and for an angle of attack range which allow the appearance of strong non-linearities, see pitching moment coefficient on Figure 11.
The evaluation of the method is done for three different dynamic pressures which correspond to the cruise plus the extremes seen in flight for that Mach number. For each dynamic pressure, a flexible polar is calculated with the rapid flexibilisation method and compared to the polar obtained by the CFD/CSM model. The comparisons are done for the global aerodynamic coefficients of the wing and for the local distributions of lift and pitching moment along the wing span.

For medium dynamic pressure (cruise), the aeroelastic effect is already significant, Figure 11. The lift and pitching moment slopes in the linear zone decrease as expected but the behavior in the non-linear zone is no more a simple scaling of the rigid polar. Clearly, the linear methods cannot predict such evolution. The rigid and the flexible polar cross at a particular angle of attack. For this point, the deformed shape (Flight shape) is the shape used in the rigid database (Reference shape).

The rapid method predicts very well the flexible polars on both linear and non-linear zones for the lift coefficient as well as for the pitching moment coefficient.

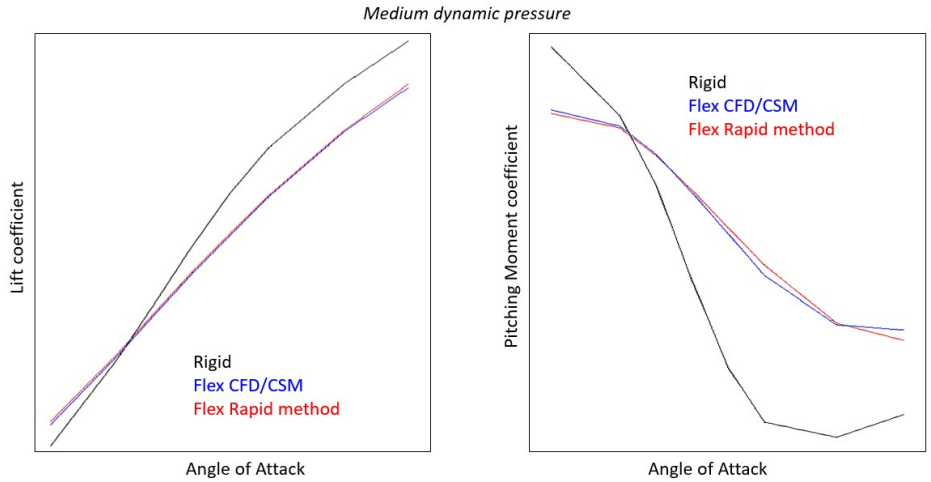

Figure 11 : Global lift and pitching moment coefficient vs. angle of attack, medium dynamic pressure

The flexible distributions are also very well predicted, Figure 12 to Figure 14 for 3 different angle of attack. Some differences are visible especially on the pitching moment distribution. Nevertheless the overall accuracy is very good with respect to the other sources of uncertainties like CFD mesh deformation, mapping of the forces on FEM nodes or extraction of the distributions from the CFD results.

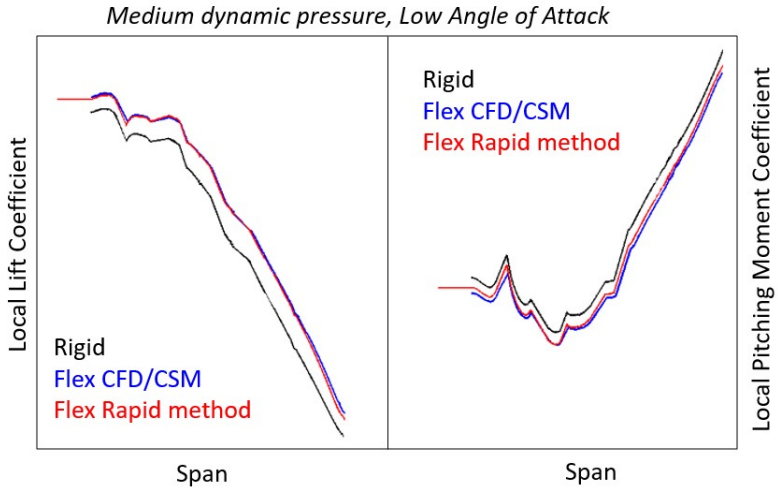

Figure 12 : Local lift and pitching moment distribution, medium dynamic pressure and low angle of attack

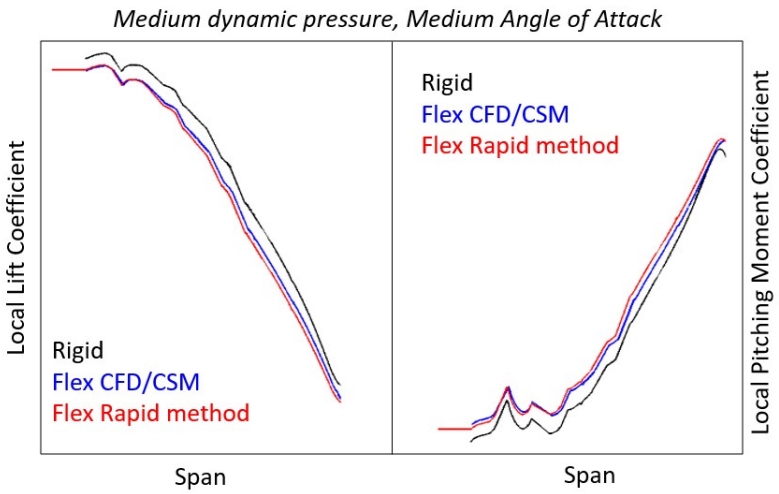

Figure 13 : Local lift and pitching moment distribution, medium dynamic pressure and medium angle of attack

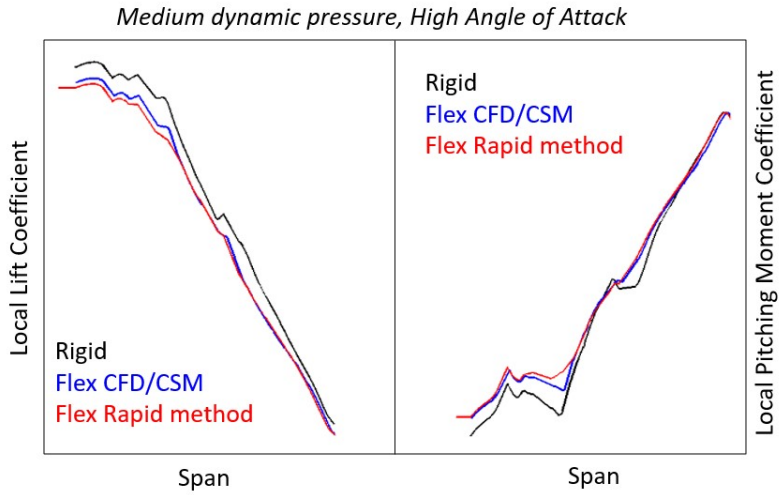

Figure 14 : Local lift and pitching moment distribution, medium dynamic pressure and high angle of attack

Now, the results for a lower dynamic pressure are presented, Figure 15. As expected, the aeroelastic effects on the global aerodynamic coefficient slopes is reduced; compared to the medium dynamic pressure. An interesting effect is appearing in the non-linear zone. Above a certain angle of attack and up to the end, the flexible and rigid polars are superimposed. For that dynamic pressure, at low incidence, the flexible wing has a highest twist than the reference shape; the lift produced by the sections is higher. Then, the angle of attack will increase and the twist will decrease due to the structural deformation. When angle of attack reaches the non-linear zone, each section will be progressively limited by its maximum lift capability. Globally, the flexible polar will 'saturate' to the same value than the rigid polar.

The prediction of the rapid method is still very good. Some differences appear on the pitching moment coefficient at high angle of attack whereas the lift coefficient is very well predicted. It could be attributed to the lever arms used to compute the moment. In CFD/CSM, the lever arms between each CFD nodes and the reference aerodynamic point are updated to take into account the deformation of the wing. In the rapid method, the lever arms are constant, calculated with the Reference shape. If needed, this change of lever arm could be taken into account without problem.

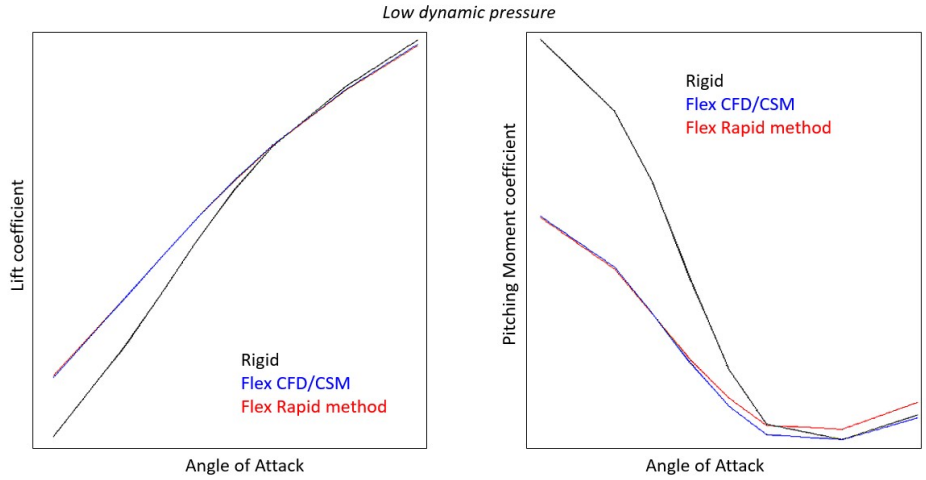

Figure 15: Global lift and pitching moment coefficient vs. angle of attack, low dynamic pressure

The distributions for the low dynamic pressure and 3 angle of attack are shown in Figure 16 to Figure 18. The 'saturation' effect is fully developed on the last incidence. The flexible distribution remains superimposed with the rigid one. The prediction of the rapid method is very good. Even for the last incidence. The fact that, the prediction is good on the distributions but not as good on the global pitching moment coefficient, confirms the problem with the lever arms.

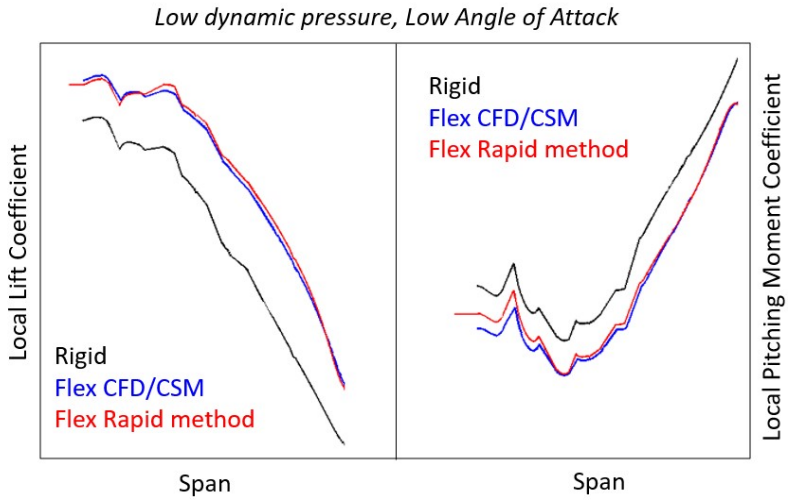

Figure 16 : Local lift and pitching moment distribution, low dynamic pressure and low angle of attack

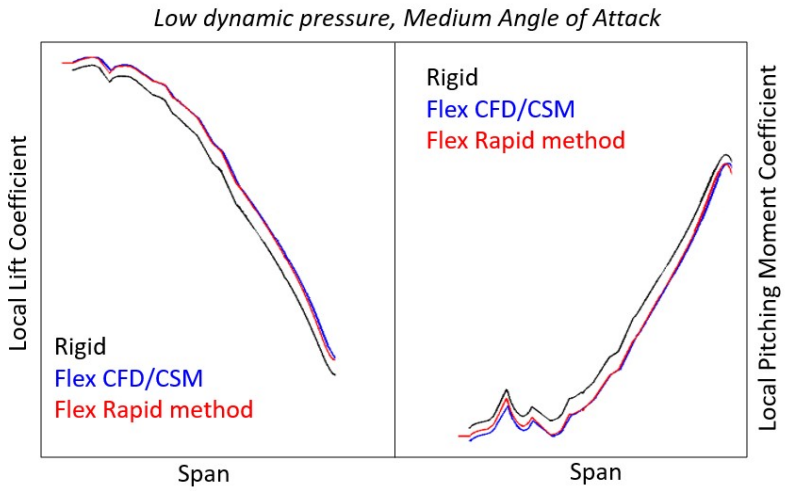

Figure 17 : Local lift and pitching moment distribution, low dynamic pressure and medium angle of attack

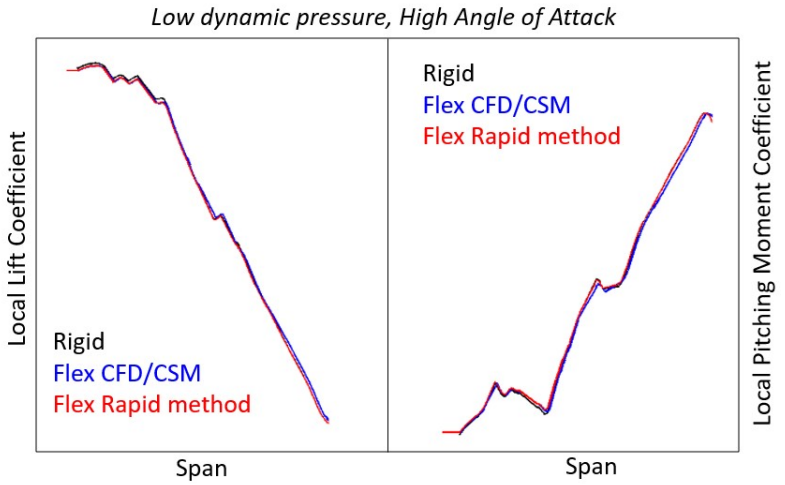

Figure 18 : Local lift and pitching moment distribution, low dynamic pressure and high angle of attack

Finally, the results for the highest dynamic pressure are presented here. The effect of flexibility on the lift and pitching moment coefficient slopes is, as expected, higher than for the medium dynamic pressure, see Figure 19. For high dynamic pressures, the deformation of the wing is quite large. The effective angle of attack will be lower than the one in the rigid case. The flexible polars have not yet entered in a deep non-linearities whereas the rigid polars have reached this non-linear region. As for previous cases, the rapid method gives excellent results. Nevertheless the approximation of the lever arms in the rapid method degrades again the results on the pitching moment coefficient. On this particular dynamic pressure, the wing deformation was so high that the CFD/CSM process was not able to converge at high incidence, probably due to some mesh deformation problems. The rapid method still continues to deliver results which seem to have a physical meaning even if there are not validated by a high fidelity method. It shows that the rapid method is not only accurate but also very robust.

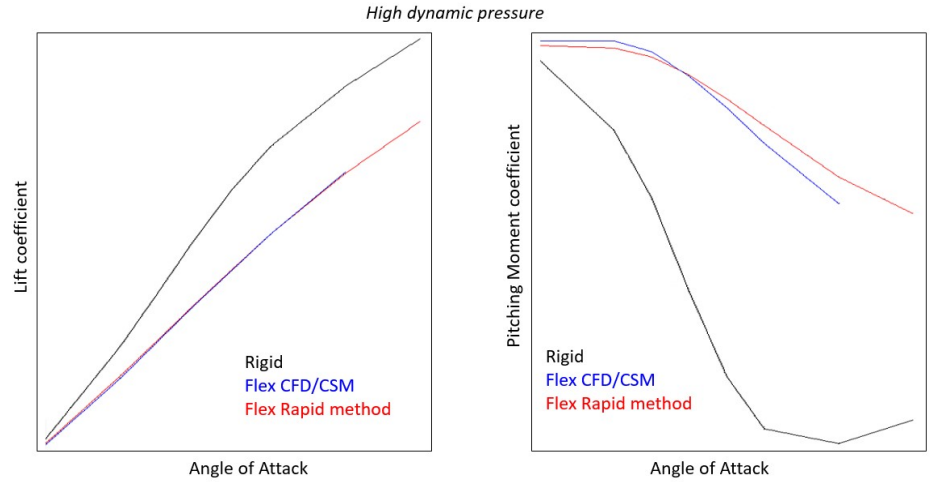

Figure 19 : Global lift and pitching moment coefficient vs. angle of attack, high dynamic pressure

The results for the distributions are shown on Figure 20 to Figure 22. The same level of accuracy is reached for this dynamic pressure, regardless of the angle of attack.

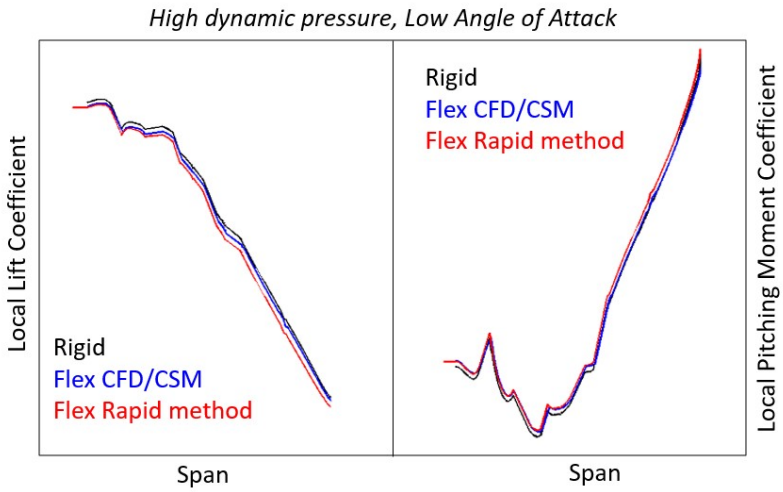

Figure 20 : Local lift and pitching moment distribution, high dynamic pressure and low angle of attack

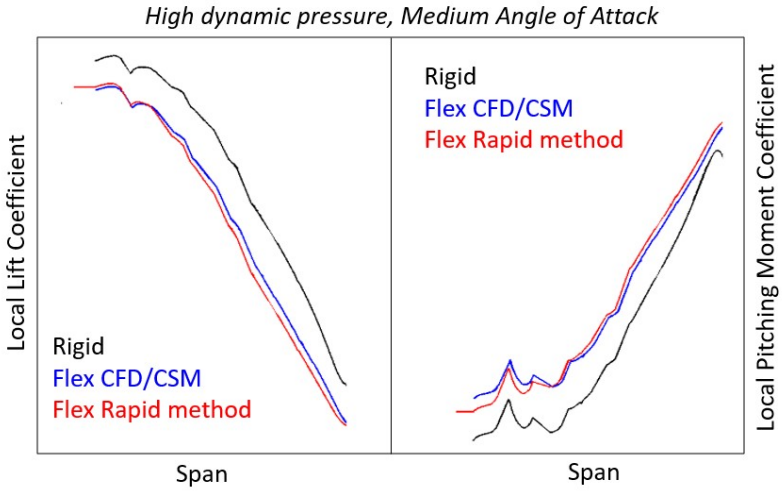

Figure 21 : Local lift and pitching moment distribution, high dynamic pressure and medium angle of attack

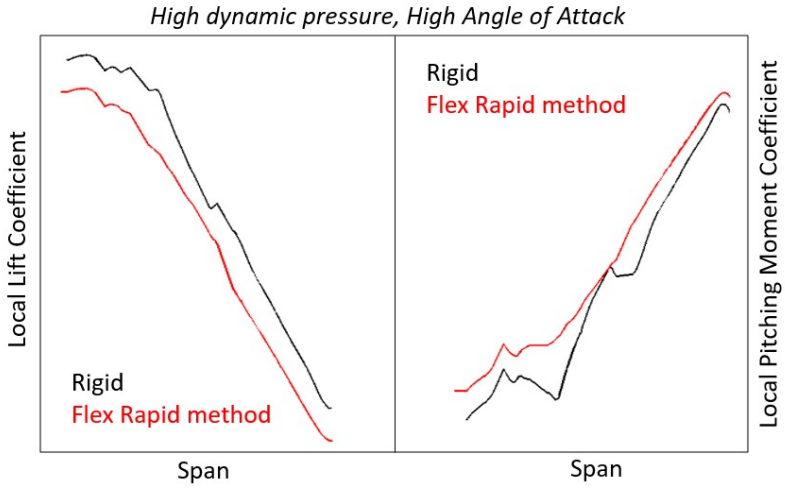

Figure 22 : Local lift and pitching moment distribution, high dynamic pressure and high angle of attack

6 CONCLUSIONS

A rapid method has been proposed to solve the static aeroelasticity problems taking into account the transonic aerodynamic non-linearities due to compressible and viscous effects. The method makes use of a pre-computed aerodynamic database which contains the 3D non-linear local lift and local pitching moment polars. The structural deformation leads to a local change of the effective incidence which is estimated using a vortex lattice method. The rapid method interpolates, in the aerodynamic database, the new local lift and pitching moment for each section of the wing with the corrected effective incidence. From wind tunnel test analysis, it has been shown that this correction is only depending on the difference of the two shapes but not on the global angle of attack of the test. A direct formulation of this delta incidence has been proposed which avoid any iteration between the VLM solver and the viscous database. This is possible only because the aerodynamic database contains already the 3D induced incidence. This rapid method has first been validated with the wind tunnel results for two known shapes. The method has been able to capture very strong non-linear effects with a very good level of accuracy. It has been then introduced in a standard static aeroelasticity loop and the results have been compared with a high fidelity CFD/CSM process. The results obtained are very good. The global aerodynamic coefficients and the local distributions have been retrieved with a high accuracy and the non-linear behavior has been captured. The method gives accurate results even when the final deformed shape is far from the reference shape used in the aerodynamic database. Nevertheless the method could be improved by taking into account the real lever arms in the calculation of the global pitching moment coefficient. This could be made by creating a database in pressure rather than in distribution and doing the integration on the fly with the correct deformed shape. This is also a smart way to take into account the effect of the wing dihedral change.
Compared to the CFD/CSM, this rapid method has shown many advantages.

1. The first one is the computational time. Once the database is created, the aeroelastic coupling is computed in less than one second; compared to several hours for the CFD/CSM. This is particularly interesting when a lot of conditions have to be calculated, like for instance a large range of mass cases or for sensitivity studies around the wing stiffness.

2. The second advantage is maybe more important. The method is very robust. It is key when a large aeroelastic calculation campaign has to be launched. For any combination of angle of attack, Mach and dynamic pressure, the rapid method has always run well and has always given results which have a physical meaning. On the opposite, the CFD/CSM is still suffering of a lack of robustness when the deformation becomes high. This is mainly due to the mesh deformation. Close to the wall, the size of the cells are very small in order to capture the boundary layer. Any strong local deformation leads to the distortion of these cells which degrade the mesh quality and sometime leads to negative volume. Recent improvements have been made for the automatic mesh repair but the robustness is still not at 100%.
3. -The last big advantage of the rapid method is its versatility. In this paper, the rigid aerodynamic database has been produced with wind tunnel or CFD results. The rapid method is able to treat any kind of aerodynamic data since it is given for a fixed shape as function of the global angle of attack. Up to now, the CFD alone is not able to give accurate results in the entire flight domain, in an industrial context. The CFD/CSM range of validity is limited by the CFD validity itself, so it will not give accurate aeroelastic results in the limit of the domain. In order to cover the entire flight domain, the Aerodynamic will necessarily be a mix of several sources: CFD, wind tunnel tests, flight tests, empirical methods… The proposed non-linear rapid method is able to handle such composite data and could deliver accurate and robust static aeroelasticity effects in the all domain.

7 WAY FORWARD

The rapid method has been applied with success to a wing in clean configuration, i.e. without any control surfaces. The aeroelastic effects on the control surface effectiveness is nevertheless a key topic. The linear methods can predict the loss of control surface effectiveness due to static aeroelasticity effects only in the linear region. But they are not applicable in the non-linear region where interactions between incidence and control surface effects become very complex. The effectiveness of control surface at high angle of attack is indeed very important for the design of Loads Alleviation Functions (LAF). Those functions are usually activated when the aircraft enters into off-design severe conditions, like 2.5G pull up. The incidence reached during these manoeuver is far above the linear zone and the linear control surface effectiveness is no more valid. As a future work, it is proposed to assess the rapid method for a non-clean wing in presence of control surface, ailerons and spoilers. It is also envisaged to extend the method to other aircraft components like horizontal and vertical tail planes. Of course the aeroelastic effects are weaker than on the wing and could be covered by linear method. Nevertheless it is always interesting, from a process point of view, to have a unique solution which can cover all the effects, on all components.

As a conclusion, thanks to its simplicity, accuracy, robustness and versatility, the rapid non-linear static aeroelasticity method could replace efficiently the CFD/CSM in many area. It opens also the door to a more intensive usage of non-linear flexible corrections within the development of an aircraft program.

8 REFERENCES

[1] Christian Agostinelli, Christian Allen and Abdul Rampurawal. "Flexible Wing Twist Optimisation using Rapid Computational Methods", 30th AIAA Applied Aerodynamics Conference, 25-28 June 2012, New Orleans, Louisiana.

[2] Livne, E., "Future of Airplane Aeroelasticity", Journal of Aircraft, Vol. 40, No. 6, 2003, pp. 1444-1450.

[3] Luis R. Miranda, Robert D. Elliot, and William M. Baker, "A Generalized Vortex Lattice Method for Subsonic and Supersonic Flow Applications", NASA Contractor Report 2865, 1977.

[4] Gabor O, Koreanschi A, Botez R, “A new non-linear vortex lattice method: applications to wing aerodynamic optimizations”, Chin J Aeronaut 29(5):1178–1195, 2016

[5] A. Grozdanov and E. Laurendeau, “Transonic Aeroelasticity using the 2.5D non-linear vortex-lattice method”, International Forum on Aeroelasticity and Structural Dynamics, IFASD 2017, 25-28 June 2017, Como, Italy

[6] “Accelerated loosely-coupled CFD/CSD method for nonlinear static aeroelasticity analysis”, Huixue Dang, Zhichun Yang, Aerospace Science and Technology 14(4):250-258, June 2010

[7] “Reduced-Order Modeling of Unsteady Aerodynamics Across Multiple Mach Regimes”, Skujins, T. and Cesnik, C. E. S., Journal of Aircraft, Vol. 51, No. 6, November-December 2014, pp. 1681-1704.